



NLR-TP-2005-193

Unstructured grid coarsening for efficient analysis of cavity backed stacked patch antennas

J.W. van der Burg, D.R. van der Heul and H. Schippers

This report has been based on a paper presented at the 9th International Conference on Numerical Grid Generation in Computational Field Simulations, San Jose, U.S.A., June, 2005.

This report may be cited on condition that full credit is given to NLR and the authors.

Customer: National Aerospace Laboratory NLR
Working Plan number: AS.1.B/AV.1.E
Owner: National Aerospace Laboratory NLR
Division: Aerospace Systems & Applications
Distribution: Unlimited
Classification title: Unclassified
July 2005

Approved by:

Author	Reviewer	Managing department
 18/7/2005	 18-07-2005	 18/7/2005



Summary

The paper is focussed on introducing grid coarsening in unstructured tetrahedral and hybrid grids which is needed to reduce the computational effort of a Computational ElectroMagnetics (CEM) analysis for patch antennas. Grid coarsening is achieved by starting from an isotropic unstructured grid where gradients in the electric field are well-resolved and choosing a direction(s) without large gradients. The paper will present algorithmic improvements, examples and experiences with grid coarsening for a patch antenna.



Contents

1	Introduction	4
2	Algorithmic improvements needed to achieve grid coarsening in a tetrahedral grid	6
3	Element transformations to recover missing edges	7
4	Examples of grid coarsening	8
5	Conclusions and recommendations	12
6	References	13



1 Introduction

Modern fighter aircraft are equipped with an increasing number of antennas in order to fulfill more and more operational functions. These are mainly related to radar, Electromagnetic Counter Measures (ECM) and Communication, Navigation and Identification (CNI), see Figure 1. The operational functions use a wide range of frequencies. If for each new operational function a dedicated conventional antenna would be added to the platform, this would have a significant detrimental effect on the aircraft performance. Conventional antennas form protuberances that affect the aerodynamic characteristics and the (radar) signature of the aircraft. To satisfy the increasing requirements on avionics functions, but to limit the aforementioned negative effects of adding conventional antennas, there is a worldwide interest in *conformal antennas*, which can fulfill multiple functions and which can be flush-mounted on or integrated in the exterior structure of the aircraft. The National Aerospace Laboratory NLR and TNO Physics and Electronics Laboratory cooperate in the project “Integration of Smart Antennas in Aircraft Composite structures” (ISAAC) to support the Royal Netherlands Air Force with advice’s regarding application of conformal antennas in present and future aircraft. The technology development in the ISAAC project is governed by the design, manufacturing and testing of three different demonstrator antennas:

- A phased array antenna with cavity-backed antenna elements, which is integrated in a composite door of an aircraft.
- A multi-layer dual frequency band antenna, which is integrated in a composite hood structure.
- An array of patch antennas mounted on a vibrating aluminum plate.

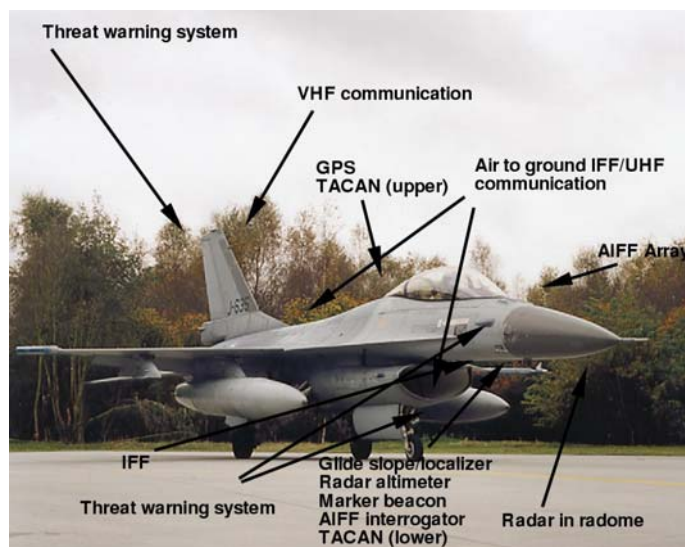


Figure 1 Antenna proliferation on typical fighter aircraft.

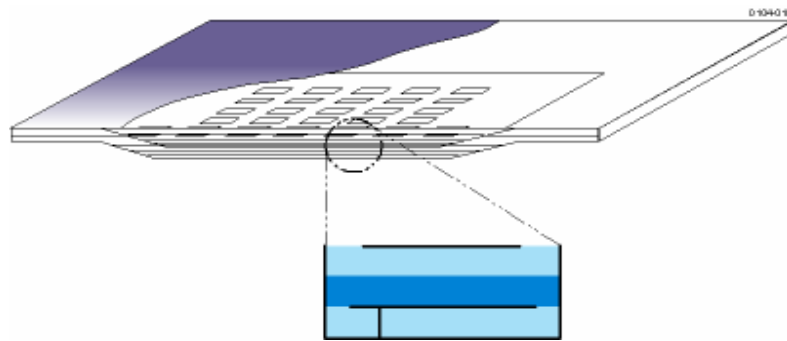


Figure 2 Layout of array of stacked cavity backed antenna elements.

The present paper addresses the generation of unstructured grids for the analysis of *cavity backed patch antenna* elements to be used in the first demonstrator antenna. The most basic arrangement for a cavity backed antenna is a single radiating strip element mounted on a cavity backed dielectric substrate. The element is excited through microstrip line, a coax connector or through aperture coupling. Although single patch cavity backed antennas have very limited bandwidth, wide band characteristics can be achieved by stacking a number of (passive) elements between layers of different dielectric material on top of the excited element (as shown in Figure 2).

The characteristics of these antenna elements can be accurately studied with the aid of a Computational ElectroMagnetics (CEM) tool, based on the full-wave solution of the Maxwell equations by means of a Finite Element–Boundary Integral (FE-BI) formulation. The unstructured grid generation algorithms of the FASTFLO CFD system (Ref. 1) are deployed to generate tetrahedral grids and surface triangulations for the FE-BI tool that is used for the analysis of the antenna elements.

To optimize the bandwidth of the stacked patch antenna element, many parameter variation studies have to be conducted to reveal the influence of e.g. patch sizes and stack layer thickness' on the input impedance. In order to limit the required computational resources and to reduce the turn-around time for the complete analysis it is a prerequisite to control the shape and size of the finite element locally.

In this paper more background information will be given on newly introduced algorithms to achieve a grid coarsened tetrahedral grid. Experiences with a cavity-backed antenna will be reported. In addition the potential of grid coarsening is illustrated for a three-dimensional high-lift application.



2 Algorithmic improvements needed to achieve grid coarsening in a tetrahedral grid

The unstructured grid generation algorithms are based on a constrained Delaunay Tetrahedralization (CDT) method. A Constrained Delaunay Tetrahedralization is best characterized as a set of tetrahedral elements bounded by a given surface triangulation. In a CDT method a boundary recovery algorithm is needed to restore the connectivity of the boundary surface triangulation in the tetrahedral grid. Delaunay-type unstructured grid generation has the property that the bounding surface triangulation is lost in the tetrahedral grid connectivity. In numerical experiments conducted for stacked patch antennas it has been observed that the main showstopper for creating a tetrahedral grid with grid coarsening is the boundary recovery algorithm.

Grid coarsening in a tetrahedral grid is defined by means of a line source that specifies a coarsening factor in the direction along the line source. Grid coarsening is then introduced in both the surface triangulation and the tetrahedral grid. Similar approaches can be found in (Refs. 2, 3, 4).

The boundary surface triangulation for the stacked patch antenna consists of a number of surface planes that are relatively close together. In literature there is evidence that for a surface triangulation that is formed by planes, the creation of a tetrahedral grid with coarsened tetrahedral elements becomes an insurmountable problem (Refs. 5, 6, 7). Quote from Ref. 5: "Constrained Delaunay tetrahedralization has the unusual status of being NP-hard only for degenerate inputs". In other words the creation of a tetrahedral grid starting from a pre-defined degenerate bounding surface triangulation cannot be solved in polynomial time $O(n_T n_s)$, where n_T and n_s represent the number of nodes in the tetrahedral grid and the surface triangulation. In this framework by degenerate is meant: a bounding surface triangulation is degenerate if it has five (or more) nodes on a common sphere.

This degeneracy occurs for instance in case the nodes of a surface triangulation are uniformly distributed on the antenna planes. The NP-hardness would imply that the creation of a tetrahedral grid for this surface triangulation could not be achieved in polynomial time, which seems to be somewhat counter-intuitive. This difficulty can be overcome by locally changing the bounding surface triangulation, for example by adopting a randomly small shift of nodes along the surface plane (Ref. 8). As a result a valid tetrahedral grid can be produced.

Now by introducing grid coarsening, tetrahedral elements will become ill-conditioned and the number of significant digits will reduce (see also Ref. 9). As a result the bounding surface triangulation becomes degenerate. The idea is now to find out whether it is still possible to produce a coarsened tetrahedral grid for a stacked patch antenna type configuration (that consists of planes).



The boundary recovery algorithm basically consists of a number of intersection algorithms. To recover a bounding surface triangulation it is necessary to introduce extra nodes, which are intersection points, usually referred to as Steiner points (see also Ref. 7). Firstly, the missing edges of a bounding surface triangulation are recovered by deriving the intersection with tetrahedral elements and introducing additional points at the location of intersection. Missing surface triangles are recovered by deriving intersections with tetrahedral elements. Finally, newly introduced intersection points need to be removed or moved away from the surface. It should be mentioned, that a surface edge swap algorithm exists that recovers missing edges by locally changing the surface triangulation by swapping edges. This algorithm can only be employed, however, at non-planar geometries.

Guideline for the improvement of the boundary recovery algorithm has been to avoid the introduction of Steiner points. In a Delaunay-based grid generation algorithm it is possible to minimize the number of edge-to-triangle intersections employed by transforming tetrahedral elements. This will be discussed in more detail in the next section.

It should be noted that for an advancing front algorithm it is more difficult to minimize the number of edge-to-triangle intersections. For the creation of each tetrahedral element a number of edge-to-triangle intersections needs to be performed.

3 Element transformations to recover missing edges

In order to explain these element transformations consider a missing surface edge, i.e. an edge of the surface triangulation that is not represented in the tetrahedral grid. First step is to verify whether the swapped (or reflex) surface edge is represented in the tetrahedral grid. If this is the case the associated tetrahedral elements are derived. The idea is to transform these tetrahedral elements in order to recover the missing surface edge. In case the swapped edge is not represented in the tetrahedral grid, the missing edge still needs to be recovered by introducing Steiner points.

Pre-requisite is that the nodes of the missing edge are also represented in the tetrahedral elements. If this is the case the missing edge can be recovered by means of a tetrahedral element transformation (described below). In case the nodes of the missing edge are not represented, repeated transformation algorithms can be foreseen (not described in this paper).

To explain the tetrahedral element transformation algorithms some notation needs to be introduced. Signify an (existing) swapped edge as e_N when the edge is associated to N tetrahedral elements. As an example, edges with four and six associated elements are illustrated in Figure 3.

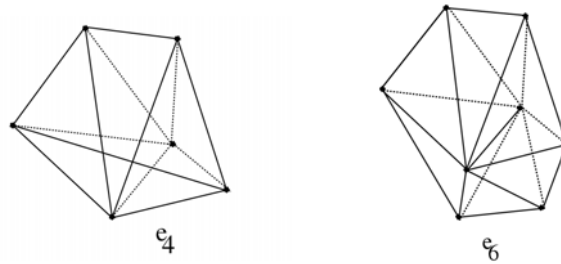


Figure 3 Example of an edge associated to four (left) and to six (right) tetrahedral elements.

A swapped edge that is associated to 3, 4, 5 or 6 elements can be transformed using the transformations described in (Ref. 9). For a swapped edge associated to 7, 8, 9 or 10 elements the below listed transformations have been introduced:

$$\begin{array}{ll}
 e_7 \rightarrow e_3 + e_6; & e_8 \rightarrow e_3 + e_7 \\
 e_7 \rightarrow e_4 + e_5; & e_8 \rightarrow e_4 + e_6 \\
 e_9 \rightarrow e_3 + e_8; & e_{10} \rightarrow e_3 + e_9 \\
 e_9 \rightarrow e_4 + e_7; & e_{10} \rightarrow e_4 + e_8
 \end{array}$$

A transformation can be successfully performed only if the volumes of the transformed tetrahedral elements stay positive. As a result of the transformations new edges and tetrahedral elements have been formed. Experiences with these newly introduced transformation algorithms now will be reported.

4 Examples of grid coarsening

The electromagnetic properties of a cavity backed patch antenna are studied by solving a finite element discretisation of the Maxwell equations within the antenna volume (see also Ref. 10). Tetrahedral elements are used, because these allow a straightforward definition of intrinsically solenoidal shape functions.

To accurately resolve the impedance/ frequency relation of the antenna the computational method has to capture the strong gradients in the electric field that occur in the vicinity of and orthogonal to the edges of the metallic patches, when the antenna is excited near the resonance frequency. Hence, there are possibilities to coarsen the grid in the direction where gradients are expected to be small, like for instance along the edges of the antenna patches.

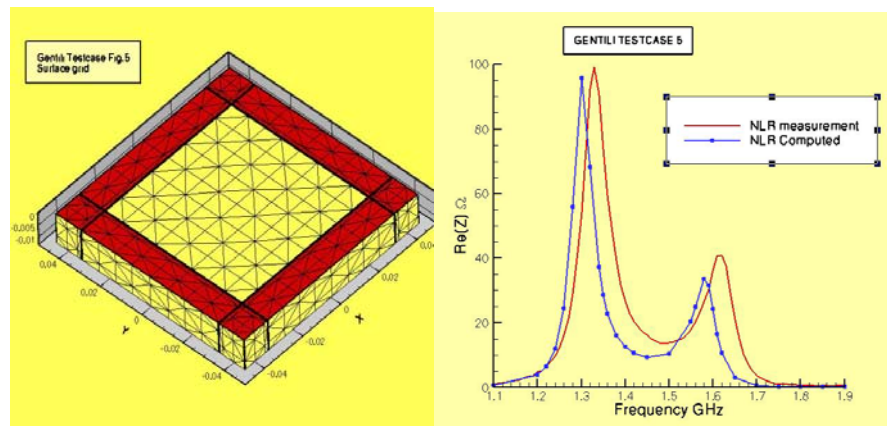


Figure 4 Example of a surface triangulation for the stacked patch antenna based on a multi-block structured grid with stretched cells near the antenna patch boundaries (left). Computed and measured antenna input impedance.

To match the antenna element with the feed line, the antenna input impedance has to be accurately known. Figure 5 shows a computational grid for a stacked patch antenna, where the upper patch is coplanar with the ground plane (see also Ref. 10). The red (dark in black and white) zone in Figure 5 is the aperture of the antenna, where the magnetic current distribution is expanded in linear solenoidal basis functions. On the edges of the patches the magnetic currents vanishes. If the grid is not sufficiently refined near the edges of the patches, the edge is 'smeared out' and the patch is effectively elongated. Because the resonance frequency of the antenna element is directly related to the dimensions of the patch this artificial elongation leads to a severe under prediction of resonance frequency. Figure 5 (right) shows the computed and measured input impedance for the antenna element.

Initially, for conformal antenna applications tetrahedral meshes were constructed by subdivision of structured hexahedral meshes, taking advantage of the anisotropy by increasing the aspect ratio of the hexahedra. However, for these structured meshes grid refinement can not be controlled sufficiently and grid resolution is wasted. On the other hand, unstructured tetrahedral meshes are generally nearly isotropic and cannot take advantage of the anisotropy in the solution. Adaptive unstructured grid refinement would lead to a locally isotropic refined grid. The ability to directly coarsen the unstructured mesh along the edges of the patches would combine the advantages of both approaches.

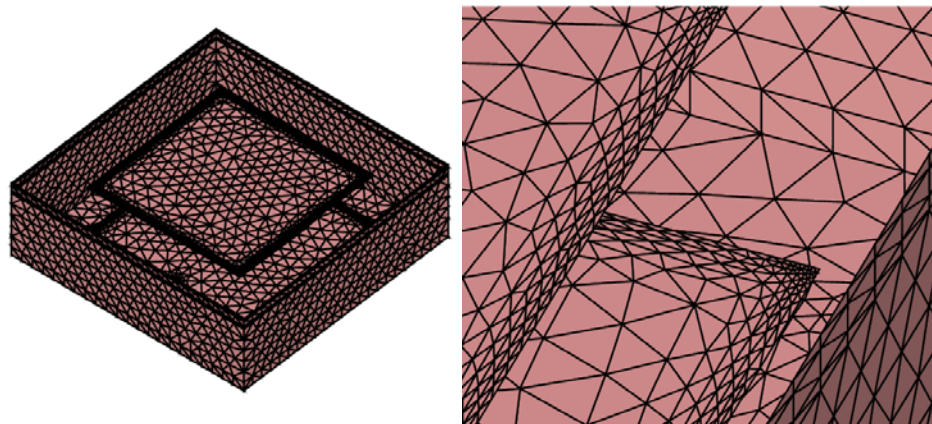


Figure 5 Surface triangulation for the rectangular box and the stacked patch antenna with a grid coarsening factor of 7 along the edges of the antenna patches. Zoom of the edges of the antenna patches (right).

The initial surface triangulation for the cavity backed patch antenna configuration comprises of a rectangular box that is subdivided by 4 parallel horizontal planes and one vertical plane. The internal planes define the boundaries between the different dielectric slabs of the stack and the position of the antenna patches and the feed. The internal planes decompose the computational volume in 6 separate non-connected tetrahedral parts. The thickness of each of the upper three dielectric slabs is in the order of 5% of the cavity depth. In order to reduce the grid size at the edges of each antenna a line source with a grid-coarsening factor of 7 has been specified (see also Figure 5) which is currently the maximum achievable value for this type of antenna configuration. Specification of larger coarsening factors would typically lead to a breakdown of the boundary recovery algorithm.

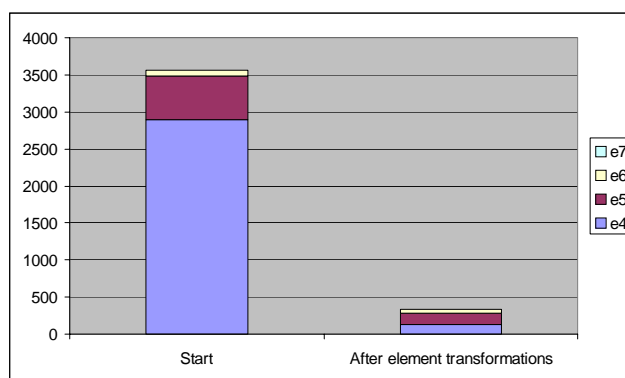


Figure 6 Number of missing edges for which a swapped edge exists at the start and after the tetrahedral element transformations e_4 , e_5 , e_6 and e_7 .

In Figure 6 it can be observed that initially the number of missing edges for which a swapped edge exists is in the order of 3500. It can be concluded that by employing tetrahedral element transformations this number is substantially reduced, namely to 335. As a result a large number

of edge-to-triangle intersections are avoided in the boundary recovery algorithm and a valid tetrahedral grid is produced.

The surface triangulation consists of 19100 nodes and the final tetrahedral grid has approximately 100.000 nodes. The CPU-time to generate the tetrahedral grid is 65 seconds on an SGI workstation. Without the use of the tetrahedral element transformations it was not possible to create a tetrahedral grid.

Part of the algorithms to create a grid coarsened unstructured grid has been developed for high-lift aircraft configurations. For studying high-lift flow in a reasonable time frame it is essential that the number of nodes in hybrid (prismatic/tetrahedral) grid is reduced. This research has partly been carried out in the frame of the EU funded Eurolift II project focussed on High Lift Aerodynamics (Ref. 11).

There is a need as well to introduce structured type surface triangles at the leading edges of the wing elements in order to enhance accuracy at these locations. These surface triangles are beneficial for the local accuracy since the resulting prismatic elements will satisfy a central symmetry property. Furthermore, the structured type surface elements enable to specify a transition line more easily. Examples of grid coarsening applied to high-lift configurations can be found in (Ref. 3, 4), where it was chosen to adopt non-structured type cells at the leading edges.

In Figure 7 examples of grid coarsening with triangular structured surface elements are shown. Grid coarsening in spanwise direction has been introduced at the wing leading edges (slat, main wing and flap) of a high-lift wing. At these locations flow gradients are expected to change rapidly in chordwise direction, but slowly in spanwise direction. This is due to a high local surface curvature that exists in chordwise direction in contrast to the spanwise direction.

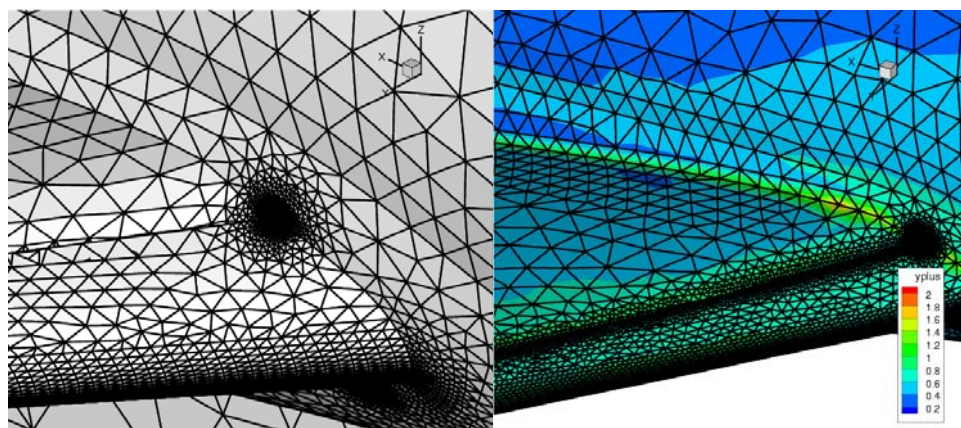


Figure 7 Examples of a surface triangulation of the KH3Y high-lift configuration with a spanwise grid coarsening factor of 8 (left) and 6 (right) Computed y^+ distribution on the resulting hybrid grid (right).



5 Conclusions and recommendations

In the paper it has been demonstrated that it is possible to introduce grid coarsening in an unstructured grid for a patch antenna and a high-lift configuration. There is a clear need to produce unstructured grids with coarsened cells for stacked patch antenna applications. Without grid coarsening the turnaround time of a full wave CEM analysis would become prohibitively large. By introducing grid coarsening a significant reduction in turnaround time can be achieved making CEM studies for stacked patch antennas feasible. The turnaround time basically will depend on the amount of grid coarsening introduced.

The maximum attainable coarsening factor in numerical experiments considered is, currently, in the order of 8 until 10. In a surface triangulation larger coarsening factors are feasible (up to 100). There seems to be a practical limit to which a three-dimensional unstructured grid can be locally coarsened. A challenge will be to further increase this coarsening factor for both CEM and CFD applications. Larger coarsening factors have already been demonstrated for wing alone-type configurations (in the order of 20) and additional transformation algorithms can be foreseen to support this.

Experience with isotropic tetrahedral grid generation with the newly introduced algorithms has learned that in most cases nearly all missing edges are recovered by the newly introduced tetrahedral element transformations.

The influence of grid coarsening on the accuracy of the solution has not been investigated in further detail in this paper, but forms part of currently ongoing National and European research projects. It can be foreseen that in case the grid-coarsening factor becomes large, the accuracy of the discretization is negatively influenced. New solver algorithms could be foreseen to account for this effect. For example, a similar correction to a viscous flow discretization stencil is made to account for the local wall-normal stretching of an unstructured grid in order to resolve a viscous boundary layer.



6 References

1. Burg, J.W. van der, Weide, E.T.A. van der, “Short turnaround time turbulent flow computations for complete aircraft configurations”, 23rd ICAS congress, Toronto, September 2002. Also issued as: NLR Technical publication 2002-270, see web-site: www.nlr.nl.
2. Yamakawa, S., Shimada, K., “High quality anisotropic tetrahedral mesh generation via ellipsoidal bubble packing”, Proceeding of the 9th International Meshing Roundtable, New Orleans, Louisiana, USA, 2000.
3. Eliasson, P., CFD improvements for high-lift flows in the European project Eurolift”, AIAA Applied Aerodynamics, AIAA-2003-3795, June 2003.
4. Mavripilis, D.J., “The development of unstructured grid methods for computational aerodynamics”, presented at the Cornell University, Ithaca, New York, September 2002.
5. Grislain, N., Shewchuk, J.R., “The strange complexity of constrained Delaunay triangulation”, In Proceedings of the 15th Canadian Conference on Computational Geometry (CCCG'03), pages 89-93, 2003.
6. Ruppert, J., Seidel, R., “On the difficulty of triangulating three-dimensional nonconvex polyhedra”, Discrete & Computational Geometry, Springer Verlag,, Vol. 7, pp. 227-253, 1992.
7. Miszka, B., Ryan, G., Gain, J., Hultquist, C., “An application of tetrahedrisation to from-point visibility”, Technical Report CS-04-12-00, Dept. of Computer Science, University of Cape Town, 2000.
8. Kryszl, P., Ortiz, M., “Variational approach to the generation of tetrahedral finite element meshes”, International Journal for Numerical Methods in Engineering, 2000.
9. Burg, J.W. van der, “Tetrahedral grid optimization: towards a structured tetrahedral grid”, in conference proceedings of the 7th International Conference on Numerical Grid Generation in Computational Field Simulations, Whistler, Canada, 2000. Also issued as: NLR Technical Publication 2000-343, see web-site www.nlr.nl.
10. Gentili, G.G., Garcia-Castillo, L.E., Salazar-Palma, M., “Green’s function analysis of single stacked rectangular microstrip antennas enclosed in a cavity”, IEEE Transactions on Antennas and Propagation, Vol. 45, No. 4, April, 1997.
11. Eurolift II, European High Lift Programme II, Description of Work, Annex B to contract GRD-2004-502896, January 2004.